

Wairua 2 Land Speed Vehicle Downforce: Moving Surface Boundary Layer Control Airfoils vs. Conventional Airfoils

Marie-Laure Gras¹, Franck Degan²

École de l'air et de l'espace, Salon-de-Provence, 13661, France

Ioan I. Feier³

United States Air Force Academy, USAF Academy, CO, 80840, USA

Land speed vehicles can benefit from additional downforce to allow more grip during the traction limited phase of acceleration or braking. Ideally downforce should be controllable and variable throughout the speed range. Downforce can be obtained via conventional wings or by more novel methods such as moving surface boundary layer control (MSBLC) wings. MSBLC is a generalization of the Magnus effect. The work here investigated conventional airfoils and several MSBLC airfoils in which the entire surface was moved in a treadmill conveyor belt fashion. Results were studied for Reynolds numbers up to 1×10^7 per meter, and Mach number up to 0.67. MSBLC concepts included a simple belt airfoil composed of two rollers of different diameters, and more complex airfoil shapes made up multiple arcs and straight segments. Coefficients of lift, drag, and moment are presented for various angles of attack and velocity ratios (surface speed to freestream speed). MSBLC airfoils are shown to significantly improve L/D ratios, delay stall, and promote more docile stall behavior. These airfoils are compared to more conventional cambered airfoils for controlling the downforce on the Wairua 2 streamlined land speed vehicle, intended for speeds in excess of 500 mph. A conventional supercritical winglet design was chosen for the Wairua 2 land speed vehicle, to reduce complexity and meet build timelines.

I. Introduction and Motivation

Land speed vehicle records are established on straight line acceleration courses. In the U.S. typical land speed record attempts at the Bonneville Salt Flats are now limited to a five statute mile acceleration course. The CMR team (Cook Motor Racing, Auckland NZ) has several records in the Wairua 1 streamliner vehicle, with documented course exit speeds in excess of 318 MPH at Bonneville. Figure 1 shows the existing Wairua 1 vehicle at Bonneville. Prior work shows that for traction limited land speed vehicles to achieve record setting speeds on shorter courses, it is prudent to enhance traction by adding downforce during the early traction limited part of the run, and then remove unnecessary downforce and drag once the vehicle is no longer traction limited [1]. Hence, an aerodynamic system with variable downforce would be optimal: high downforce at lower speeds, and lower downforce (but enough for stability) with correspondingly lower drag at higher speeds. Even for longer courses where traction is less of a consideration, having control over the downforce to eliminate lift can improve safety, balance the vehicle, and allow adaptability to changing grip conditions of the salt or dry lake bed surface. The surface can vary between dry and high grip to wet with standing water. Additionally, downforce can also be used to control the tire loads during the run and provide shortened and emergency braking.

¹ 2nd Lt., French Air and Space Force.

² 2nd Lt., French Air and Space Force.

³ Associate Professor, Department of Mechanical Engineering, AIAA Senior Member.

Controlling the downforce in motorsports is similar to controlling lift in aerospace. For their main wings, aircraft control their lift by controlling the angle of attack (AOA), or by controlling the geometry of the wing via slats and flaps. At low speeds leading edge slats and trailing edge flaps increase the effective camber of the wings, creating more lift for a given AOA. In addition, at low speeds higher AOA values are used as compared to cruise speeds. In many motorsports races active aerodynamics such as dynamic AOA and movable slats and flaps are banned or severely restricted. In the fastest land speed racing classes active aerodynamics are not restricted. For instance, Fig. 2 shows vehicles such as Carbinite and Flashpoint which include active aerodynamics and are capable of 400 mph or above. The aerodynamic performance of these two vehicles is unknown as aerodynamic data was not found in the open literature. From a practical perspective, design complexity is a limitation in land speed racing due to limited testing and short competition cycles. Multi-element dynamic wings were initially considered for Wairua 2 (i.e. flaps and slats, or multiple main elements), but they were quickly excluded from the design space due to the short developmental time prior to manufacturing and the added complexity of the mechanisms that would require actuators and kinematic design. Additionally, the downforce winglets are relatively small and thin, making mechanisms and actuators harder to package in the wings themselves.

The Wairua 2 vehicle is currently being built with its current progress shown in Fig. 3. The final integration of the downforce winglets and actuators is expected in the first half of 2024. The goal for Wairua 2 is to be the fastest piston-powered, wheel-driven vehicle with record attempts taking place at large salt flats such as Salar de Uyuni (Bolivia) which can enable much longer 10-12 mile track lengths as compared to Bonneville. Such longer tracks ameliorate the need of massive downforce to create grip, since longer distances would be available for acceleration. Instead, the primary benefit of winglet downforce would be to control vehicle trim and ensure that that the vehicle is always in a downforce configuration without any lift.

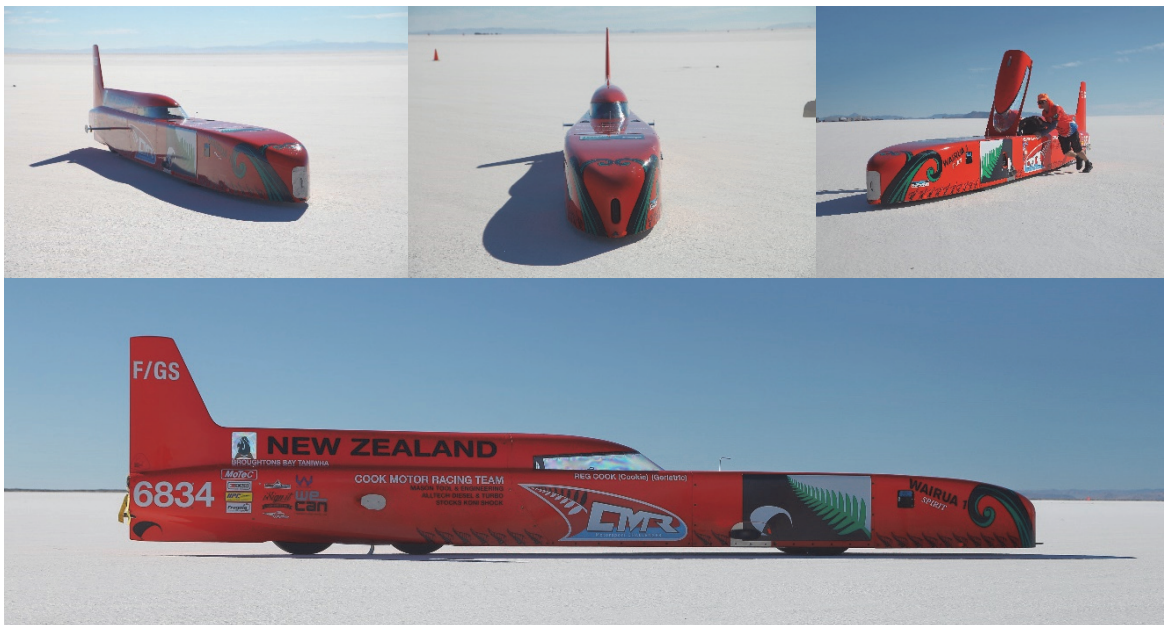


Fig. 1 The Wairua 1 vehicle shown at a 2018 Bonneville Salt Flats land speed record competition from different views. The vehicle has achieved Bonneville speeds up to 318 mph. The Wairua 2 design [2] is a similar streamliner shape but with a different wheel layout, cockpit shape, and tail geometry. Fig. 3 shows the progress of Wairua 2 construction.

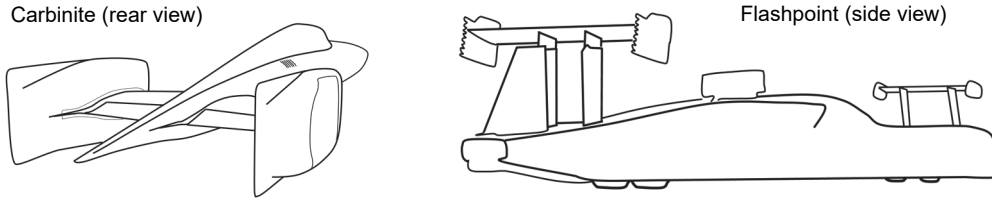


Fig. 2 Downforce land speed vehicles with adjustable wings: the Carbinite (left) and Flashpoint streamliner (right). Carbinite uses a variable camber wing (flap) and Flashpoint incorporates variable AOA for the front and rear downforce wings.



Fig. 3 The Wairua 2 streamliner vehicle shown during construction and dyno testing (December 2023).

A. Design Options: Conventional Wings vs. MSBLC Wings

Two design concepts were pursued - conventional wings and MSBLC⁴ (moving surface boundary layer control) wings. A comparison of the two concepts is shown in Figure 4 with the airfoils oriented in a downforce configuration as they would be on a land speed vehicle.

1. Conventional wings: The conventional wings considered here were limited to single element designs, with variable AOA during the speed run. Various symmetric, cambered, and supercritical airfoils were considered.
2. MSBLC wings: MSBLC wings were analyzed in various airfoil shapes with the intent of using more advanced treadmill belt boundary motion instead of the more commonly studied airfoils with spinning cylinders [3-8]. The mechanical designs for creating boundary motion with a rolling belt are not included here because the focus is on aerodynamic characterization (i.e. the belt construction, rollers, motors or drives, guides, electrical layout, etc., are not discussed).

⁴ Also often abbreviated as MSBC (moving surface boundary-layer control).

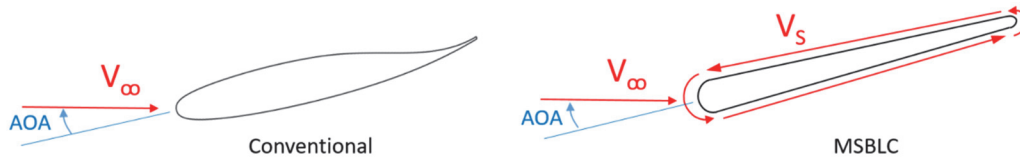


Fig. 4 Conventional downforce airfoil compared with MSBLC airfoil. The freestream velocity V_∞ is parallel to the ground with the airfoils pitched down to create downforce. The MSBLC (right) airfoil has a surface velocity V_s , shown circulating counterclockwise here to enhance downforce.

At low speed the vehicle is tractive force (grip) limited and a high vehicle downforce is the primary winglet requirement, with low drag being secondary. At higher speeds, drag becomes a larger concern than downforce, since the vehicle is no longer traction limited. Winglet pitching moment is always of tertiary importance and will not influence tire loads significantly, since the winglet is relatively small and the vehicle has a long wheelbase.

B. Introduction to MSBLC Wings

Conventional airfoils and wings have been well studied and are not summarized here. MSBLC (moving surface boundary layer control) airfoils are much rarer. Hence, an introduction follows in this section. MSBLC or controlled momentum injection has been studied for the past two hundred years, beginning with the highlight of the “Magnus effect” by German physicist Gustav Magnus, professor at the University of Berlin between 1834 and 1869 [9]. This effect showed the influence of a rotating body when immersed in a fluid flow – specifically that a rotating body can create a force which is perpendicular to the flow direction. The most notable examples are found in sports such as soccer and baseball where the spin of the ball creates a curve in the trajectory. The perpendicular force could be oriented in the lift, downforce or lateral directions. The well-documented Magnus effect can control the aerodynamics of spinning cylinders, spheres, and other bodies. The Magnus effect and its more general MSBLC application is one of only many boundary layer control (BLC) methods [10].

The Magnus effect can be approximated by the Kutta-Joukowski theorem [11-12], where the increased circulation caused by a spinning a body can create lift. Generally, the Kutta-Joukowski⁵ theorem states that

$$L' = \rho_\infty V_\infty \Gamma = \rho_\infty V_\infty \oint \vec{V} \cdot d\vec{s} \quad (1)$$

where L' is the lift per span (N m^{-1}), ρ_∞ is the freestream fluid density (kg m^{-3}), and Γ is the circulation - which can be evaluated using a closed path line integral around the airfoil of the component of the local velocity \vec{V} in the path direction $d\vec{s}$. Although the Kutta-Joukowski theorem’s derivation was originally limited for specific inviscid airfoil conditions⁶ its mathematical form and its Magnus effect perspective is illustrative for the purposes here – i.e. it suggests that increasing circulation can increase lift. For a cylinder creating a Magnus effect, the circulation Γ can be approximated as $\Gamma = 2\pi\omega r^2$ for instance, where ω is the rotation rate (rad s^{-1}) and r is the cylinder’s radius (m). Spinning cylinders can enhance lift, but their drag is also high. More streamlined airfoil applications of the Magnus effect are known to improve L/D (lift to drag) ratios, e.g. spinning cylinders at the leading edge, trailing edge, or elsewhere along an airfoil. More generally, as the study of aerodynamics has advanced, moving the surface of an arbitrary aerodynamic body has been generalized and is currently named “MSBC” or “MSBLC” instead of the “Magnus effect”, with the original Magnus effect nomenclature typically being reserved for isolated spinning cylinders or spheres. The MSBLC surface driven shear is a viscous effect that can increase lift. The lift increase could be interpreted in the inviscid sense to be caused by the increase of circulation Γ around the body, but also in the viscous sense to be caused by the reduction of stall due to reduction of boundary layer separation.

During early aeronautics Magnus effect interest grew. For instance, Auguste-Jules-Joseph Lafay studied the rotation of cylinders with different surfaces [13]. His research showed a significant decrease in pressure as the cylinder’s

⁵ Note that the name of Russian scientist Никола́й Егорович Жуко́вский (Nikolay Yegorovich Zhukovsky) is often transliterated as Zhukovsky, Joukowsky, Joukovsky or Joukowski.

⁶ Technically Martin Kutta and Nikolay Joukowsky only considered two-dimensional, steady, incompressible potential flow around airfoils with a cusped trailing edge and “any application calling for greater generality might refer to a trailing edge condition” [36].

rotational speed increased. Whereas Lafay studied the effect of air around a rotating cylinder, Prandtl [14] investigated the effect of momentum injection on cylinders plunged in water through kinetographic pictures. As water movements are easier to distinguish compared to air, Prandtl's research focused on the flow around the cylinder and more specifically how the boundary layer detached itself from it. While two eddies can be perceived on the stationary cylinder, only one is observed beneath the rear of the rotating cylinder. The moving surface enhanced boundary layer attachment. Favre [15] applied the concept directly to airfoils through his moving extrados' wing. His device was composed of a belt and multiple straps causing part of the leading edge and one surface to move in the direction of the flow at a desired speed. His research exposed the delay in the boundary layer's detachment to angles of attack up to 90° thereby increasing lift. The attached boundary layer also caused the suppression of the turbulent flow behind the wing.

It is only in the 1990's that additional research was completed. V. J. Modi [3-8] was one of the main contributors to recent MSBLC research. His experimentations were composed of multiple shapes such as flat plates, rectangular prisms and airfoils in which he implemented moving cylinders in various locations to study their influence on the lift and drag they caused according to the velocity ratio of the cylinder to the fluid [7]. His research showed great promise in the domains of automobile and aeronautics since his results showed a dramatic increase in lift and a decrease in drag such as Favre had shown through the reattachment of the boundary layer to the wing. Beyond the effect of the cylinder's location, Modi and Yokomizo [5] also studied the effect of the various surfaces that these cylinders could have on the same parameters. Twenty years later, their research was expanded further to more complex airfoils such as the NACA 23018 [16], the NACA 0012 [17] and the NACA 0010 [18] - which concluded with an improvement in the aerodynamic performance due to the MSBLC addition.

Patkunam et al. [19] and Szulc et al. [20] conducted similar experiments to Favre's with moving section of the extrados on NACA 0021 and NACA 0012 airfoils. Their research resulted in the same conclusions as had Modi's: a significant increase in lift and a decrease in drag from which aeronautics could greatly benefit. Szulc went even further in his research by showing that a moving NACA 0012 airfoil top surface in transonic flow can delay separation and alter the shock wave to boundary layer interaction. This is a flow region of interest to fighter or transport jets, and incidentally the high-speed 500 mph land speed vehicle design here. Regarding motorsports, spinning leading edge cylinders were proposed recently for Formula SAE racecar multi element downforce wings [21].

Nevertheless, all these past contributions were limited to a partially moving surface of an airfoil. However, what would happen if the entire surface of the airfoil was moving? Only some research has been conducted. The main contributions are from Sedaghat et al. [22] and Samani and Sedaghat [23] in which they study the effect of treadmill belt (or conveyor belt) motion on two NACA airfoils: 0015 and 0020. Even though their simulations were aimed at micro aerial vehicles or naval ships, they still reached similar conclusions as Modi, specifically that an important decrease in drag and an increase in lift existed as the surface to fluid velocity ratio was increased. Kazemi et al. [24] also ran their own simulations on a symmetrical airfoil they designed comparing it to the NACA 0021 with the same conclusions. Unfortunately, none of these simulations were compared to airfoils with a rotating cylinder in order to show which device is more effective.

Starting in 2017, internal studies⁷ conducted at the United States Air Force Academy (USAFA) used CFD to simulate an airfoil design for Formula SAE vehicles [25] similar to Kazemi's and compared it to Modi's trailing and leading edges' cylinder design [5]. The results showed a substantial increase in lift and a decrease in drag and preliminary work was done to build a working prototype for wind tunnel testing. The work here includes some of those earlier CFD results, expands on this initial MSBLC effort to include other airfoils, and takes the practical perspective to see if such MSBLC devices could be applied to create downforce for a land speed vehicle.

II. Computational Fluid Dynamics Methods

This section briefly describes the computational tools and methods that were used to design and analyze the designs. Geometry modeling was done via CAD (computer aided design), and performance modeling was done with CFD (computational fluid dynamics) for aerodynamics simulations. The commercial software STAR-CCM+ from Siemens was used for 2D and 3D CFD analysis. The software was used for meshing, solving, and postprocessing. When the Wairua 2 vehicle was included in the CFD model, a symmetry plane was used at the vehicle vertical centerline plane and the tires were modeled as rotating bodies with a moving ground plane. The compressible Reynolds-Averaged Navier-Stokes (RANS) steady state solver was used with fully a turbulent $k-\omega$ SST turbulence

⁷ Feier, I.I., Cecil, C., and Sentongo, S.: unpublished internal U.S. Air Force Academy reports, focusing on the CFD analysis and practical prototype construction of the conveyor belt MSBLC design presented here. However, some results and progress updates were discussed in prior conference proceedings [25].

model [26]. The models were run in parallel on 4 to 64 cores. Various domain sizes were used with either an overall freestream boundary, or a velocity inlet and a pressure outlet. The simulations utilizing a rectangular and large wind tunnel had slip conditions at the walls and ceiling in order to help eliminate the effects of boundary layer buildup and allow the simulation domain to behave more like freestream external flow. The simulations utilized cell counts of approximately 4-15 million trimmer or polyhedral cells for 3D simulations and under 1 million polyhedral cells for 2D simulations. The boundary layer mesh achieved Y^+ values under 1.0. Speeds ranged from $26.8 \text{ m}\cdot\text{s}^{-1}$ to $223.5 \text{ m}\cdot\text{s}^{-1}$, with nominal airfoil and winglet chords of 0.3 m. Generally, the MSBLC airfoils used lower speeds and the conventional/supercritical airfoils used higher speeds. 2D airfoils were simulated first, followed by more computationally intensive 3D finite length winglets, and finally 3D finite length winglets and endplates mounted on Wairua 2.

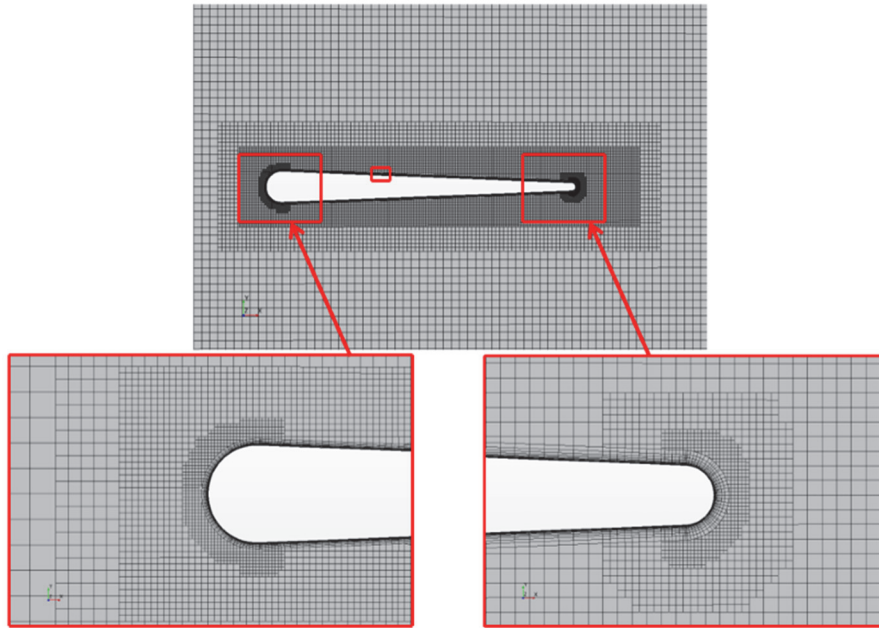


Fig. 5 2D MSBLC airfoil mesh example (trimmer cells shown)

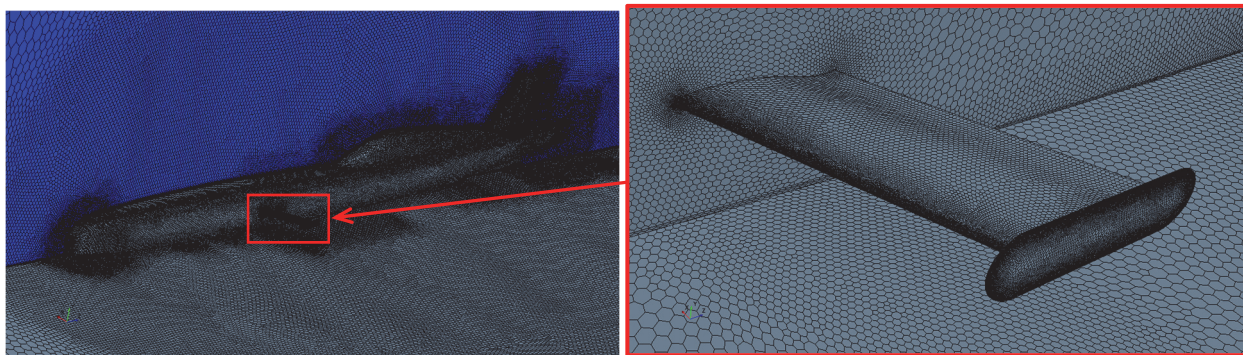


Fig. 6 3D winglet mesh example (polyhedral cells shown)

III. Results

A. 2D Conventional Airfoils

Several conventional airfoils were analyzed in 2D simulations. Among others these included a cambered Wortmann FX 72-MS-150B [27-28], a symmetric NACA 0012H [29], a cambered NACA 4412 [30], and cambered supercritical NASA NASA SC(2)-0412 [31] and SC(2)-0714 [31-33] airfoils. These are summarized in Table 1 and Fig. 7.

Table 1 Some of the conventional and supercritical airfoils considered for downforce.

Airfoil	Thickness	Camber	Notes
Wortmann FX 72-MS-150B	15%	9.7%	A high lift airfoil [27-28]
NACA 0012H	12%	None, symmetric	Modification of generic and popular symmetric NACA 0012 4-digit airfoil [29] (originally from R. M. Hicks, NASA Ames)
NACA 4412	12%	4% at 40% chord	NACA 4-digit series cambered airfoil [30]
NASA SC(2)-0412	12%	1.3% at 83% chord	Supercritical airfoil (C_L target 0.4) [31]
NASA SC(2)-0714	14%	2.5% at 81% chord	Supercritical airfoil (C_L target 0.7) [31-33]

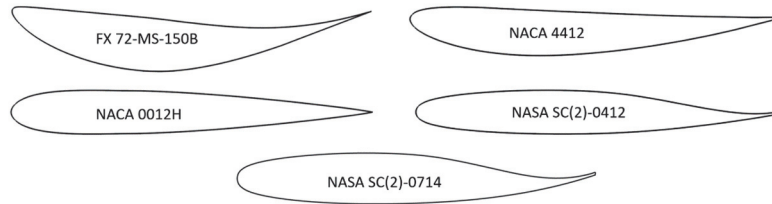


Fig. 7 Conventional (including SC supercritical) airfoils considered, shown in downforce configuration

The Wortmann airfoil and the NACA series airfoils generated high downforce at low speeds, but suffered from compressibility effects at high speeds. The suction side of the airfoils and winglets would experience supersonic flow, leading to boundary layer separation and poor performance and were thus eliminated from further study (for example the NACA 4412 winglets in Fig. 8). The NASA supercritical airfoils were selected because at a Mach of 0.667 (500 mph), they exhibited practically no supersonic flow. Specifically of the supercritical airfoils in the NASA series [31], the NASA SC(2)-0714 airfoil (14% thick, 0.7 design lift coefficient) [31-33] was ultimately chosen in order to balance low and high-speed needs. Sufficient low speed downforce at high AOA was desired, but not at expense of excessive high-speed drag when the airfoil would be in a low or negative AOA configuration.

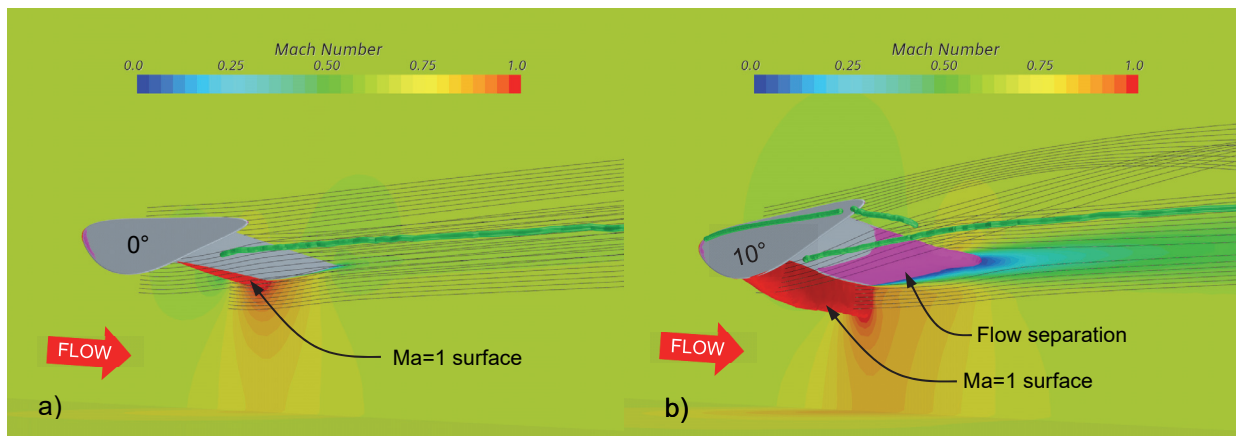


Fig. 8 NACA 4412 cambered winglets at $223.5 \text{ m}\cdot\text{s}^{-1}$ (500 mph): a) $\text{AOA}=0^\circ$, b) $\text{AOA}=10^\circ$. Mach number contours are shown on a vertical plane and the ground plane. $\text{Ma}=1.0$ (red surface) and flow separation (magenta surface) are indicated. Streamlines are black lines and vortex cores are green tubes.

B. 3D Conventional Winglets

A 3D winglet based on the NASA SC(2)-0714 airfoil was designed and sized using basic airfoil design methods to target a 2943 N downforce goal (300 kg) at $223.52 \text{ m}\cdot\text{s}^{-1}$ (500 mph). It was desired to maintain this downforce to lower speeds as well. Again, this nominal downforce goal was intended to balance the vehicle and insure that the vehicle overall did not experience any lift. The downforce from the winglets was not intended to significantly increase tractive grip. Several variations were considered. Figure 9 shows the vehicle with the final design of the winglets mounted, while Fig. 10 shows the planform view winglet geometry for the left winglet. A 25° sweep was chosen to reduce compressibility effects. A 0.3 m chord and a 0.6 m wingspan provided the necessary downforce goal at speed. The lengths are measured parallel and perpendicularly to the freestream directions, respectively. A preliminary endplate design was included to minimize wingtip vortex losses, and four vortex generators (VG) were included on the bottom suction surface to improve high AOA performance, Figure 11b.

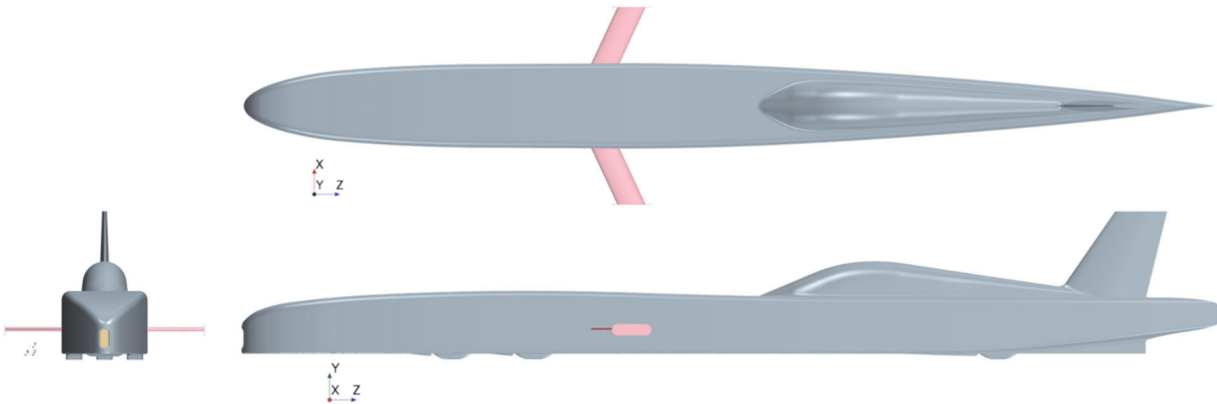


Fig. 9 Top, front, and side views of Wairua 2 with downforce winglets.

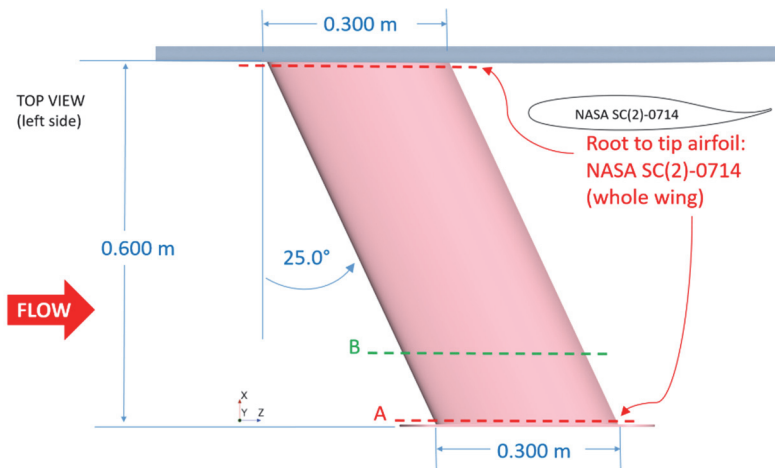


Fig. 10 Planform view of left winglet design with dimensions. The constant chord design allows for wing extensions or reductions, e.g. reducing the wingspan from A to B.

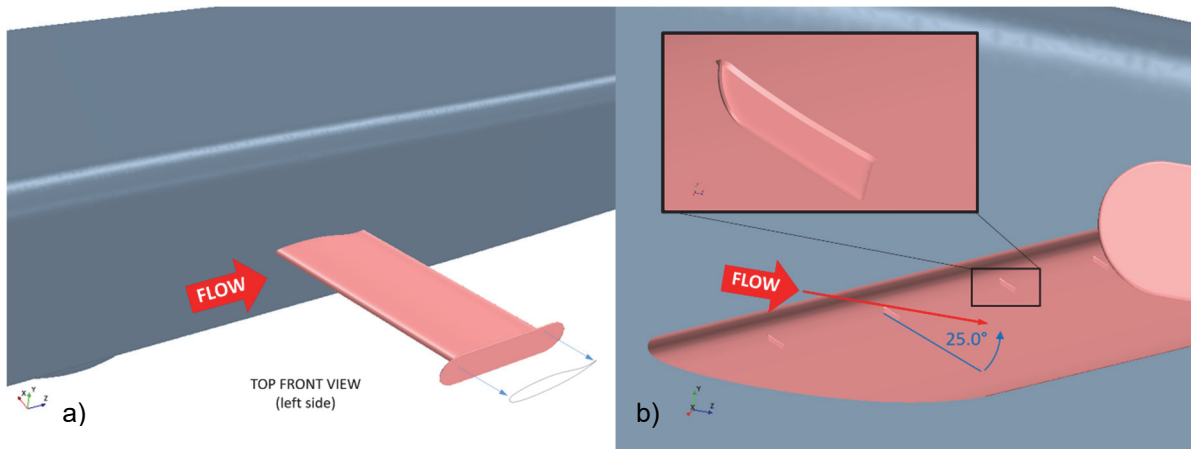


Fig. 11 Winglet design showing a) top front view, and b) the vortex generators on the suction side (bottom). The vortex generators are oriented at 25° to the freestream flow and are 20 mm long and 5 mm high.

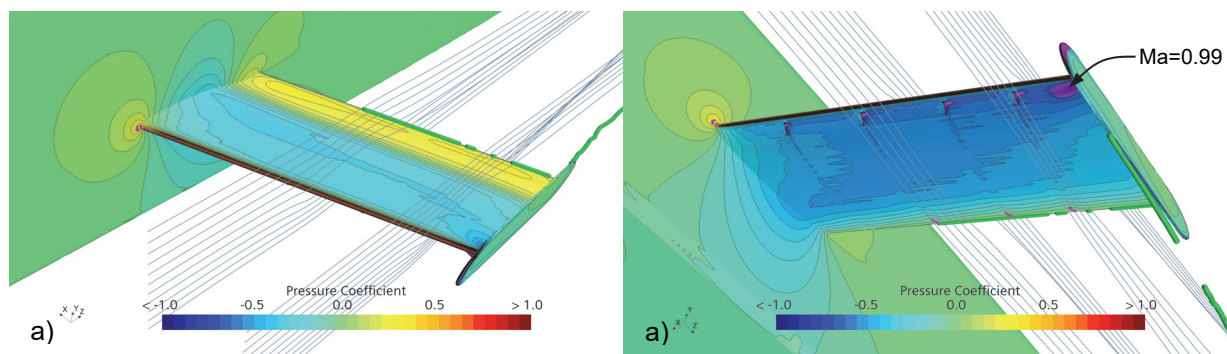


Fig. 12 a) Winglet top pressure side, b) bottom (suction) side pressure contours, with Mach=0.99 surface shown in purple (AOA 0°, 223.52 m s⁻¹). The ground effect slightly enhances suction side performance.

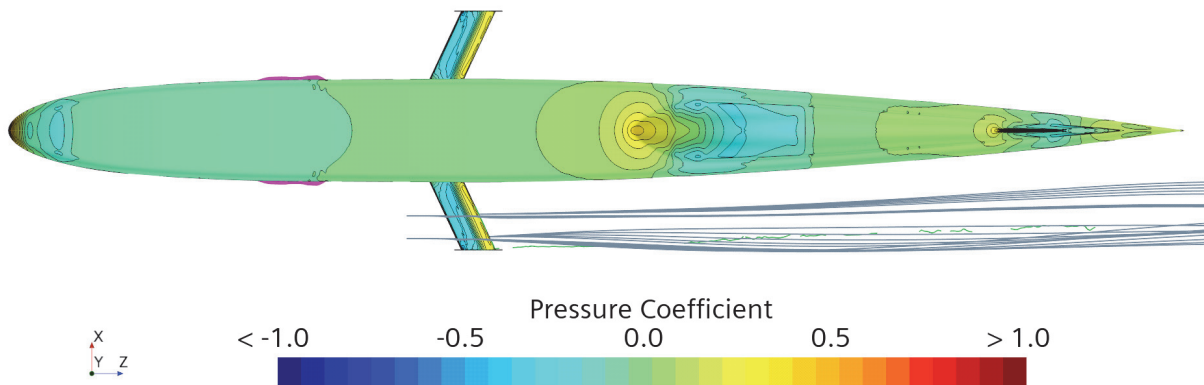


Fig. 13 Top view pressure contours for entire vehicle and winglets (AOA 0°, 223.52 m s⁻¹).

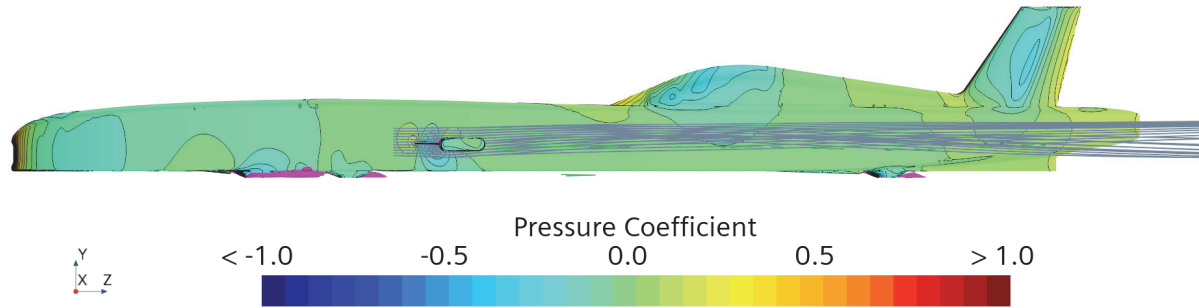


Fig. 14 Side view pressure contours for the entire vehicle with winglets (AOA 0° , 223.52 m s^{-1}).

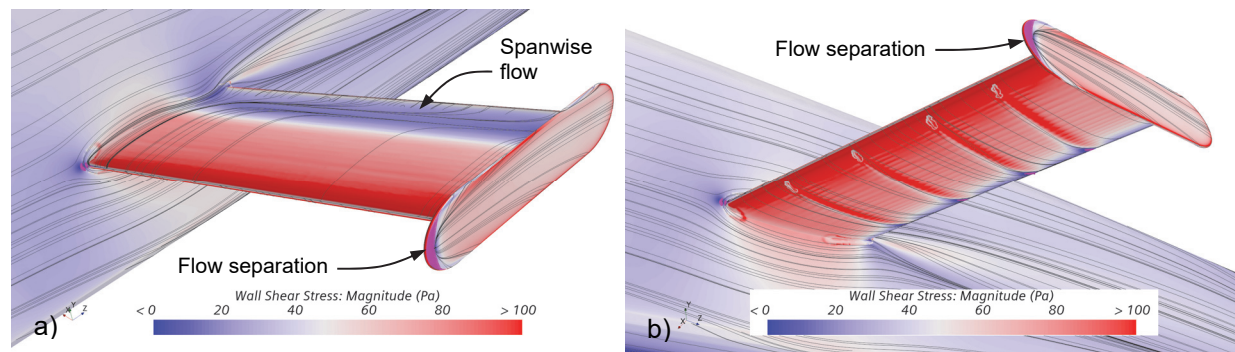


Fig. 15 Surface oil flow and shear for a) winglet top pressure side, b) bottom suction side. Some spanwise flow on the pressure side is evident, and minor flow separation at the leading edge of the endplate – shown in magenta. (AOA 0° , 223.52 m s^{-1})

The design in Figures 12-15 is at AOA= 0° and 223.52 m s^{-1} and generates 3016 N of downforce (102% of target) with 194.4 N of drag⁸, or a downforce to drag ratio of 15.5. This corresponds to a C_L of 0.416 (based on winglet planform area) and a C_D of 0.190 (based on winglet frontal area). The winglet sizing was purposely chosen to allow the wing to operate at low AOA and thereby low drag at the vehicle's top speeds, while reserving higher AOA for lower speeds. For instance, at 111.8 m s^{-1} (250 mph) and AOA= 12° the winglets are at incipient stall, but still generating 2343 N of downforce with a 230 N drag penalty (C_L of 1.292 based on winglet planform area). Whereas, at this lower speed the downforce is only 80% of the desired target, this condition still provides a reasonable downforce to drag ratio of 10.2. The winglets could be increased in size (i.e. by span extensions as suggested in Fig. 10) to provide more downforce at lower speeds at the expense of more drag. The winglets should avoid stall since stalling one winglet before the other could lead to an undesirable rolling (and yaw) moment.

The pressure coefficient contours for the AOA= 0° and 223.52 m s^{-1} condition are shown in Figs. 12-14 with representative streamlines around the winglet. The flow is well attached, and the endplate reduces the wingtip vortex. The supercritical design keeps flow subsonic, and only a small region shown in Fig. 12b on the suction side near the wing tip approaches sonic velocity. Only slight flow separation is observed at the leading edge of the endplate as shown in Fig. 15. Oil flow visualization (surface streamlines) and surface shear in Fig. 15 demonstrate well-behaved flow, but with some spanwise flow on the pressure side in the last 20% of the wing chord, where shear is also low. This spanwise flow is confined near the surface in the boundary layer. The vortex generators create increased shear in their wake (Fig. 15b).

⁸ Note that the Wairua 2 simulations were performed for atmospheric conditions representative of Salar de Uyuni (Bolivia): 3657 m elevation, 6°C (279.15 K), 0.805 kg m^{-3} density, whereas the MSBLC simulations were performed for sea level standard atmosphere conditions.

C. 2D MSBLC Airfoils

Several MSBLC airfoils were studied using 2D CFD as shown in Fig. 16 to understand their fundamental behavior vs. conventional airfoils. The simplest was a 0.3 m chord, 10% thick design made up of a 0.030 m diameter leading edge roller and a 0.008 m diameter trailing edge roller, with the geometry shown in Fig. 16a. This “conveyor belt” airfoil would be the easiest to mechanically implement. Additionally, a Joukowsky 15% symmetric airfoil and a NACA 6412 12% cambered airfoil were also included, both with optional flaps (Fig. 16b to 16e). All the airfoils were constructed from an assembly of straight line and constant radius arc segments in order to allow the CFD solver to assign tangential velocity specifications locally to each segment. Although the airfoils are shown horizontally in the figure for convenience, in a vehicle application V_∞ would be parallel to the ground and the airfoil would be pitched up or down relative to the airflow. Figures 17-20 show C_L , C_D , and C_M results, while Figs. 21 and 22 show some insight into the effect of MSBLC on the surrounding pressure field and streamlines.

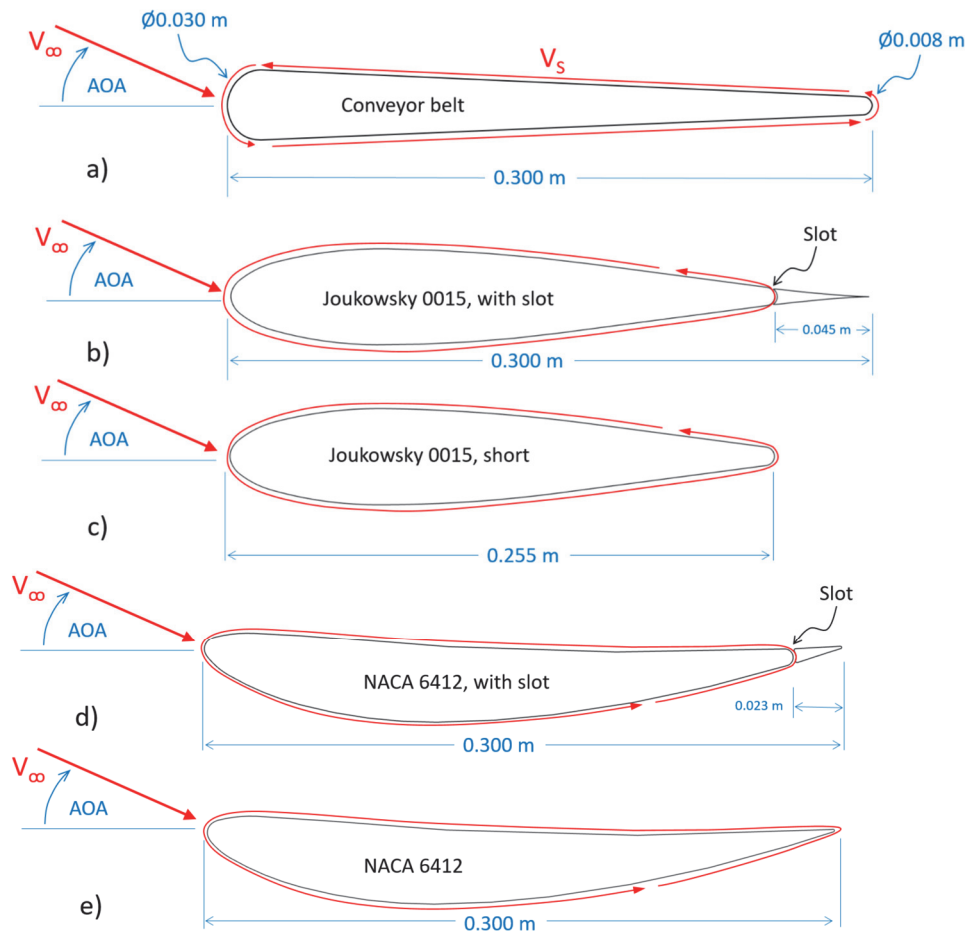


Fig. 16 MSBLC airfoils investigated: a) conveyor belt design utilizing 10% thick airfoil, b) Joukowsky symmetric 15% thick airfoil with slot (unpowered length of 45 mm or 15% of chord with a slot gap of 1 mm), c) Joukowsky short symmetric 15% thick airfoil, d) NACA 6412 cambered 12% thick airfoil with slot (unpowered length of 23 mm / 7.7% of chord with slot gap of 1.5 mm), e) NACA 6412 cambered 12% thick airfoil. Airfoils are shown in the downforce configuration. The velocity ratio (VR) is defined as $VR = V_s / V_\infty$, with a positive velocity ratio as shown (i.e. counterclockwise surface rotation) augmenting downforce, i.e. increasing the airfoil C_L . Positive C_L denotes downforce. The flaps (when included) had no surface velocity and did not pivot.

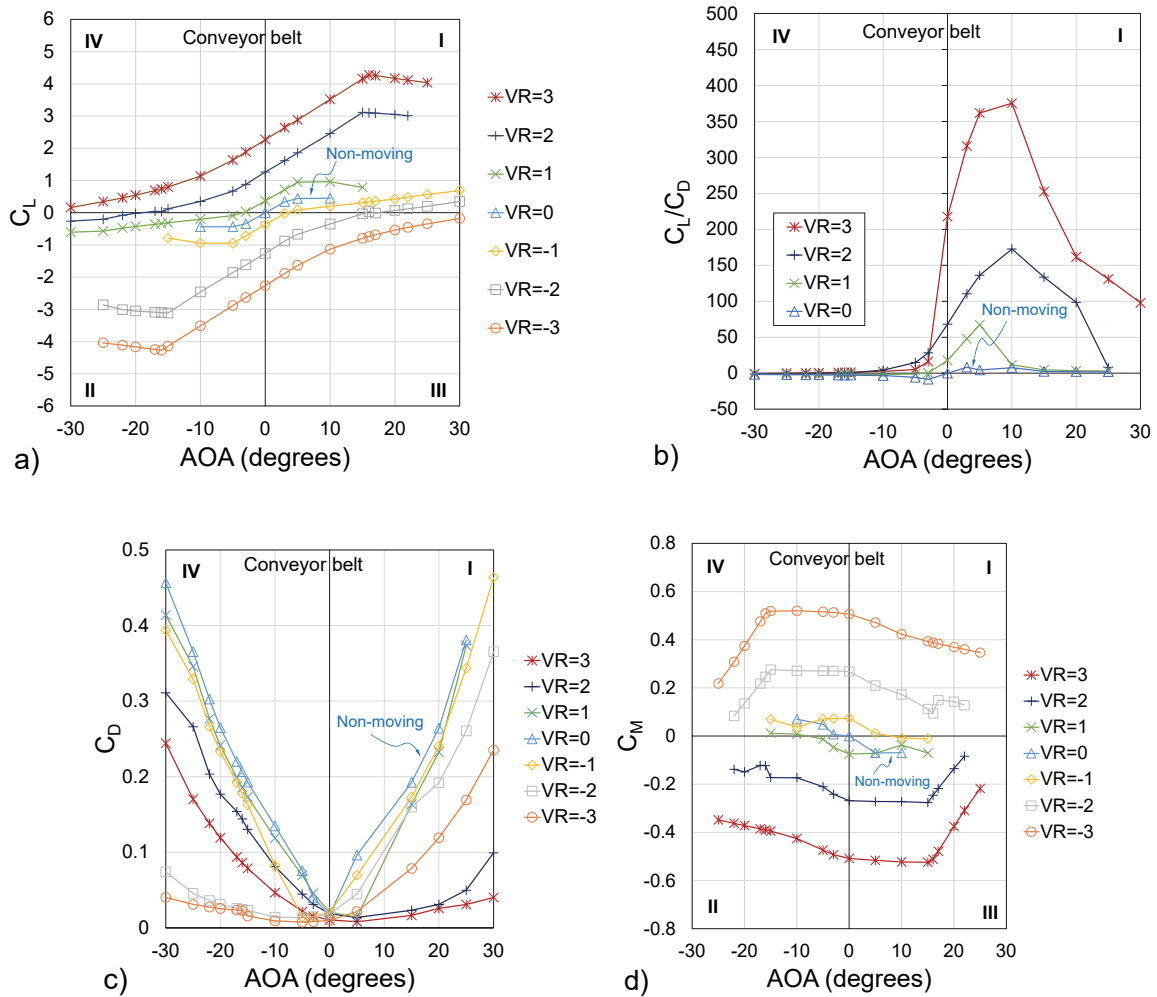


Fig. 17 MSBLC conveyor belt airfoil CFD simulations for various VR, including negative VR and negative AOA values: a) C_L vs. AOA, b) C_L/C_D ratio vs. AOA for positive VR=0, 1, 2, and 3, c) C_D vs. AOA, d) C_M vs. AOA.

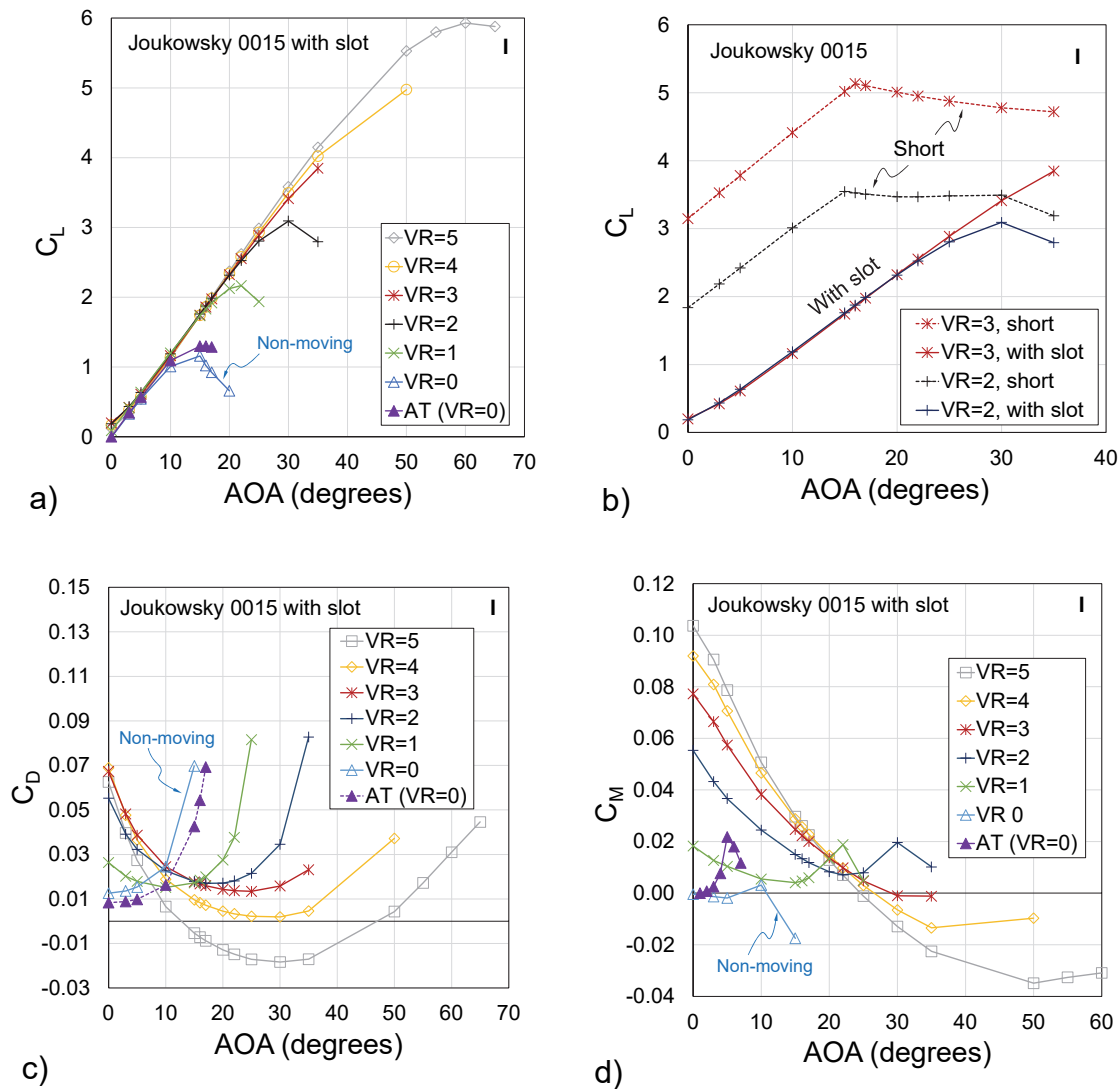


Fig. 18 MSBLC Joukowski 0015 slotted airfoil CFD simulations for various VR, shown only for positive AOA and positive VR values: a) C_L vs. AOA, b) comparison to short design for VR=2 and 3, c) C_D vs. AOA, d) C_M vs. AOA. VR=0 cases correspond to conventional non-moving airfoils.

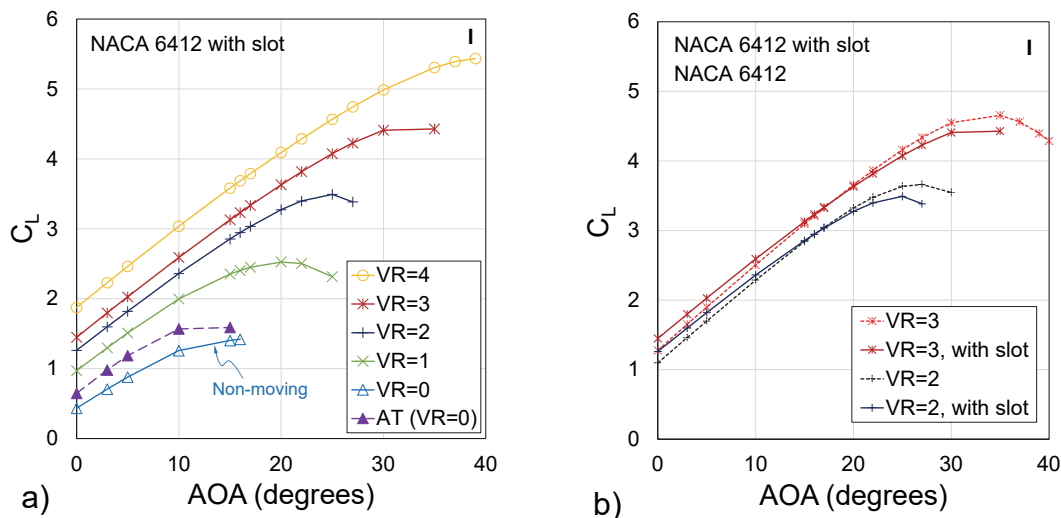


Fig. 19 MSBLC NACA 6412 slotted airfoil CFD simulations for various VR, shown only for positive AOA and positive VR values: a) C_L vs. AOA, b) comparison of slotted 6412 airfoil with regular 6412 for VR=2 and 3.

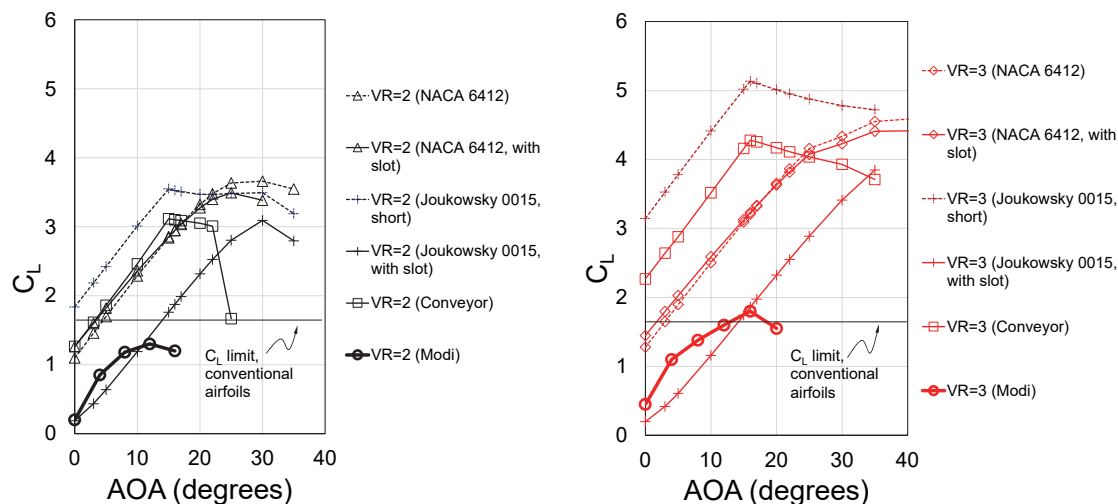


Fig. 20 Comparison of the MSBLC airfoils to Modi's spinning cylinder airfoil for VR=2 and 3, with typical $C_L \sim 1.6$ limit for conventional single element (without flaps or slats) non-moving airfoils shown for comparison. Moving the entire airfoil surface, as done here, has substantial benefit over spinning cylinder airfoils or conventional non-moving airfoils.

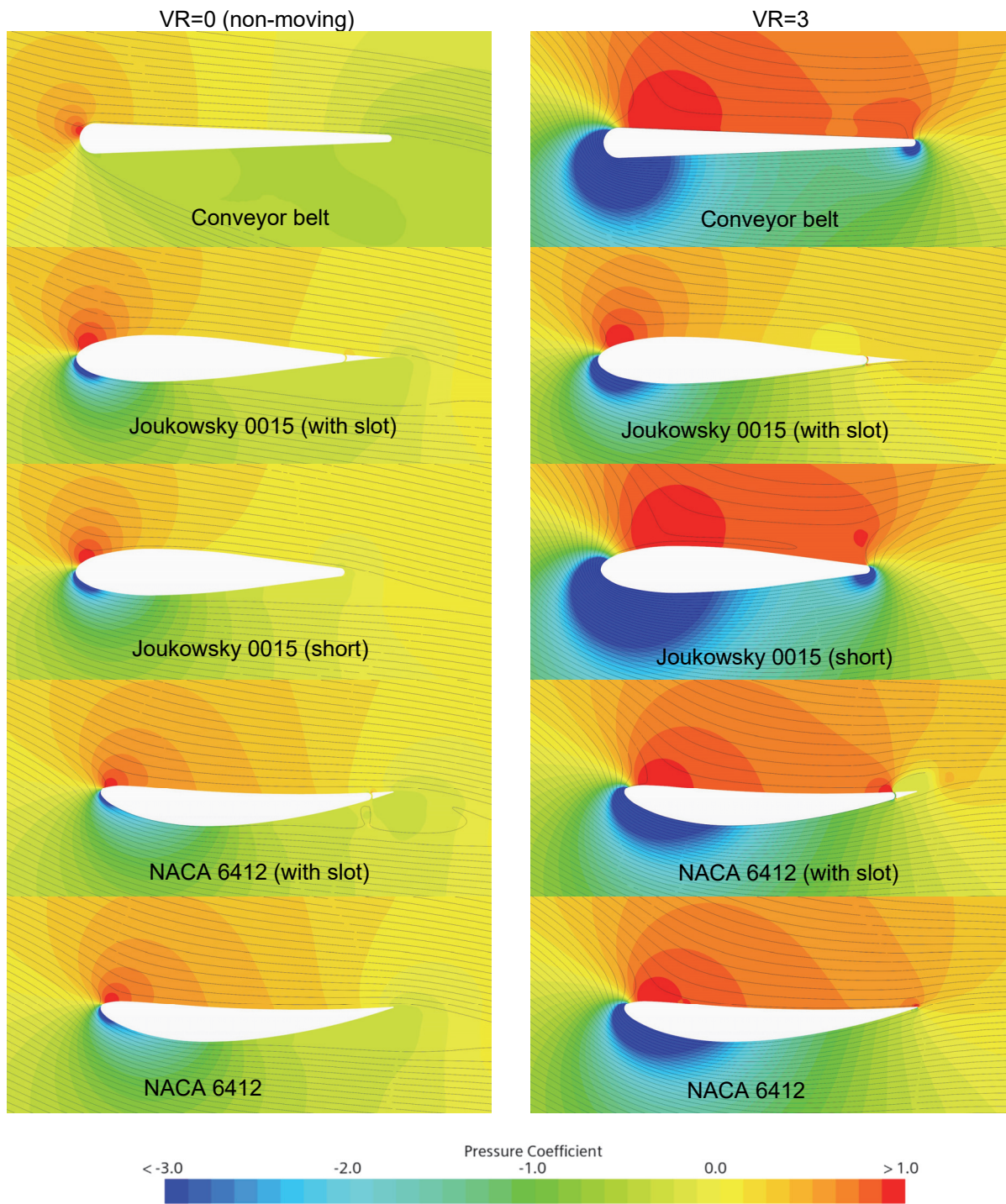


Fig. 21 Pressure contours and streamlines for MSBLC airfoils (with and without slots) for AOA=15°: VR=0 (left column) and VR=3 (right column). The VR=0 airfoils are conventional non-moving airfoils. The VR=3 airfoils have counterclockwise surface circulation which increases downforce.

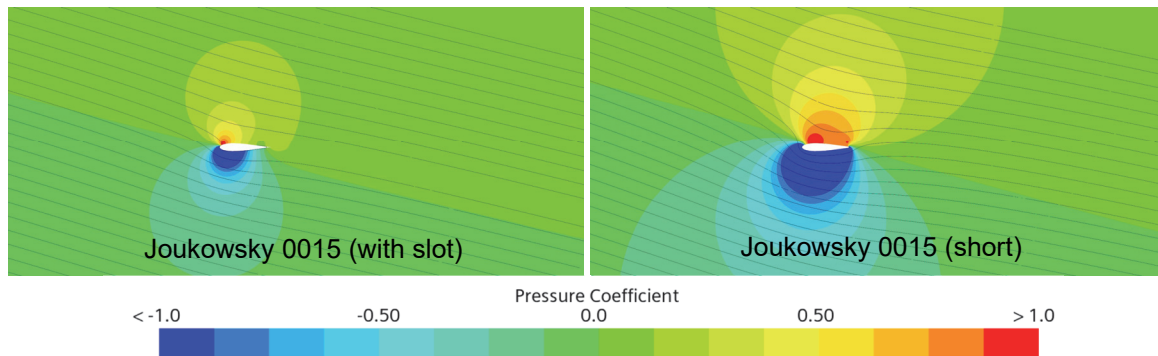


Fig. 22 Pressure contours and streamlines for the Joukowski 0015 airfoil with slot and the Joukowski 0015 short, for $AOA=15^\circ$ and $VR=3$. These are zoomed out views of the previous figure showing the far-field behaviors. The short airfoil has improved C_L due to the rounded trailing edge that allows the MSBLC effect to drag fluid from the suction to the pressure side.

Several observations can be made from the MSBLC results presented in Figs. 17-22:

- Increasing VR enhances C_L , and this is consistent for both the symmetric airfoils and the cambered NACA 6412. This effect is expected and is similar to the enhancement of lift coefficient for airfoils with spinning cylinders. The enhancements include several behaviors.
 - Stall occurs at a higher AOA. Higher VR values delay stall to larger AOA. For instance, for the conveyor belt, the stall is delayed from approximately 6° at $VR=0$ to 15° at $VR=3$ (Fig. 17a). For the Joukowski 0015 (with slot) shown in Fig. 18, stall is delayed from 15° ($VR=0$) to 60° ($VR=5$). Note the “AT $VR=0$ ” is Xfoil reference data⁹ for the stationary surface airfoil (Fig. 18-19).
 - Hence, with sufficiently high VR, the stall can be delayed until an AOA of 30 - 60° . This is a considerable improvement to the base non-moving airfoil and is competitive with multi-element airfoils, but without the added complexity and space.
 - Stall is less abrupt. Once the airfoil stalls the change in coefficients is at a slower rate for the MSBLC airfoils, particularly for the ones with rounded trailing edges.
- The aerodynamic enhancement from MSBLC is due to three main effects, which when combined lead to very high C_L and C_L/C_D ratios and the aforementioned stall delay.
 - Boundary layer separation is avoided or delayed on the suction side (bottom) of the airfoil. In Fig. 21 a comparison is presented between the airfoils at $VR=0$ (stationary non-moving surface) and $VR=3$ for $AOA=15^\circ$. At $VR=0$ all the airfoils exhibit some evidence of stall on the suction side, with the conveyor belt airfoil showing the most flow separation (leading edge stall), with the entirety of its suction side having detached flow. With MSBLC on, all the airfoils at $VR=3$ have attached flow on the suction side, with no evidence of separation. This attached flow allows the airfoils to generate a significantly greater low pressure zones near the leading edges on the suction sides.
 - Positive pressure is increased on the pressure side. Comparing the $VR=0$ and $VR=3$ cases in Fig. 21, all the $VR=3$ airfoils have larger positive pressure zones on their pressure side (top). On this side the skin surface velocity is counter to the freestream, leading to lower nearby velocities and higher pressures. The flow is in no danger of separation on this side, and the increased pressure and decreased velocity is also evident because the separation between adjacent streamlines increases.
 - Flow travel around the trailing edge enhances C_L . Compare for instance the Joukowski 0015 slotted airfoil with the Joukowski 0015 short airfoil in Figure 21. Or the NACA 6412 slotted airfoil with the plain NACA 6412. Both comparisons show added suction and pressure bubbles near the trailing edges at $VR=3$, thus enhancing downforce. The inclusion of a curvature in the trailing edge (or including a curved slot) can enhance both the suction and pressure sides. The effect is most evident in the Joukowski 0015 and a far-field view is presented in Fig. 22. The increased curvature of the streamlines and larger and stronger positive and negative pressure

⁹ Data from <http://airfoiltools.com/airfoil/details?airfoil=naca6412-il>, for $Re=500,000$ (whereas please note that the MSBLC airfoils here were simulated in CFD at $Re=551,000$).

bubbles are evident for the shortened version. Of note, if a slot is included it needs to have sufficient slot width – i.e. the NACA 6412 slot provides more benefit than the Joukowsky 0015 slot. The NACA 6412 slotted airfoil provides only marginal gains, and only at low AOA values.

Removing the trailing edge flap (i.e. Joukowsky 0015 short) appears to provide even better gains.

- Symmetric airfoils at positive AOA can have negative C_L values. This effect is common for cambered airfoils. The MSBLC velocity ratio and sign can be thought of as a tuning parameter that aerodynamically manifests itself as a variable camber that can be applied to symmetric (and nonsymmetrical) airfoils. One advantage of MSBLC lift control over the conventional AOA lift control is that with MSBLC the control may be performed faster for large wings. The rate of lift control for a vehicle can be faster if only the surface belt or motion needs to be changed instead of having to change the AOA of the entire wing (and/or the AOA of the entire vehicle or aircraft if the wing is rigidly mounted). If the inertia of the belt and drive mechanism is sufficiently small the lift vector can be flipped to downforce and back to lift fairly quickly at a wide range of AOAs. This would allow very maneuverable vehicles whose agility is not influenced by the overall vehicle pitch or yaw inertia.
- Although a pivoting axis could be used for controlling AOA as well, one of the benefits of the MSBLC concept is that downforce could be controlled by the boundary speed alone without needing additional AOA control. To obtain the most benefit, however, both the VR and AOA need to be controlled.
- Drag is not appreciably increased resulting in very high C_L/C_D ratios, as shown in Fig. 17b for the conveyor belt, for instance. However, for positive AOA drag does increase substantially if negative VR values are used. Drag values can be improved by using more streamlined airfoils such as the Joukowsky variant (Fig. 18c). Importantly, using MSBLC for the entire airfoil surface causes significant enhancement over Modi's spinning cylinder airfoils. Comparisons are shown in Fig. 20.
- High VR values with certain airfoil shapes can lead to negative drag – in other words the airfoils can generate thrust! For example for the MSBLC Joukowsky 0015 in Fig. 18c, the drag becomes negative between 14° and 36° for VR=5. This propulsive effect has been noted before [22]. Similarly, the possibility for lift at zero airspeed exists [23]. At AOA values where the C_D switches from positive (i.e. drag) to negative (i.e. thrust) the C_L/C_D ratios approach infinity. However, powering the MSBLC surface(s) would require mechanical power so any aerodynamic thrust would not be free.

The MSBLC enhancement can be thought of as a form of circulation control. Unlike traditional circulation control that is done with the momentum injection such as Coandă effect¹⁰ slot blowing [34-35], MSBLC increases the momentum and circulation using surface shear. Importantly, MSBLC directly enhances the momentum right at the surface, making MSBLC airfoils very resistant to boundary layer separation and practically immune to adverse pressure gradients. A Coandă effect device might be combined with MSBLC to provide an even more resilient circulation control design. Coandă effect circulation control using the high pressure engine exhaust from Wairua 2 was considered, but deemed to be too nascent and complex for integration.

D. 3D MSBLC Winglets

CFD studies are ongoing for 3D MSBLC winglets based on the Joukowsky 0015 short airfoil, which showed the most promising results for 2D studies. Ongoing work is to extend the MSBLC studies to higher Mach numbers to see if MSBLC can reduce the detrimental effects of shock to boundary layer interactions and increase the drag-divergence Mach number. For high Mach numbers MSBLC winglets utilizing supercritical airfoils may be necessary.

E. Limitations

Table 2 below summarizes some of the major considerations and limitations of the conventional wing and MSBLC wing approaches studied here. In particular, the MSBLC concept here has only been studied for 2D airfoils and has not been evaluated for the 3D wings that are required for a practical implementation on Wairua 2 or other vehicles. While some 3D MSBLC wings not shown here have been simulated with promising results, the MSBLC concept has serious complications at high velocity ratios. For instance, even for a relatively low speed ground vehicle traveling at $26.8 \text{ m}\cdot\text{s}^{-1}$ (60 mph) utilizing a belt traveling at a velocity ratio of 1.0 would still be mechanically difficult to implement

¹⁰ The Romanian engineer and inventor Henri Marie Coandă identified this effect in his 1910 turbine aircraft whose jet engine pushed air aft around the aircraft fuselage. Instead of the air blowing outward, it unexpectedly followed the shape of the fuselage and entrained additional air. This effect is also known as a wall jet and is used in modern aircraft blown flaps to augment lift.

as the belt would also be moving at $26.8 \text{ m}\cdot\text{s}^{-1}$ (60 mph) around its rollers. The simple two roller conveyor belt airfoil design could be mechanically implemented, but more complex airfoil shapes would require additional rollers, air bearings, vacuum surfaces, and other potential complications, particularly for concave wing surfaces like the pressure side of the NACA 6412. Increased velocity ratios are needed to take advantage of the MSBLC benefit, but at increased velocity ratios of 2, 3, 4, etc., the belt speeds would be even more extreme (i.e. 120, 180, 240 mph, etc.). Faster vehicles magnify this problem. A number of mechanical issues must be considered for such designs: how to keep the belt in the airfoil shape, belt slip, minimum bending radius, static buildup, belt fatigue due to cyclic stress, rotational inertia, sealing near static structural surfaces, and heat buildup due to friction and flexure. Including AOA mechanical control in addition to VR control would allow added flow and pitch control, but would also further complicate the implementation. Variable AOA for the MSBLC designs would be necessary to take advantage of the largest C_L and C_L/C_D ratios. The MSBLC wings would also require power to overcome the aerodynamic shearing forces and the mechanical actuation losses. Also to consider, the MSBLC winglet cannot be swept or tapered while keeping the belt's velocity vector aligned with the flow direction – at least not with simple conveyor belt kinematics utilizing conventional belts with limited stretch. While the Magnus effect has been demonstrated for full size land and flight vehicles with rotating cylinders, the authors know of no vehicle which has demonstrated the treadmill MSBLC wing concepts proposed here. Hence, the MSBLC approach is technologically risky and difficult to implement on Wairua 2.

Table 2 Conventional vs. MSBLC approaches with their current status and limitations

	Conventional approach	MSBLC approach
Speed regime investigated	111.8 - 223.5 $\text{m}\cdot\text{s}^{-1}$ (125 - 500 mph) $Re = 7.8 \times 10^5$ to 3.1×10^6	26.8 $\text{m}\cdot\text{s}^{-1}$ (60 mph) $Re = 5.5 \times 10^5$
Airfoil and/or wing studied?	Airfoil and wing	Airfoil only
Aerodynamic maturity	High	Low
Downforce control	AOA (angle of attack) control, 0° to 10° studied	VR (velocity ratio) control with VR -3 to +5 studied, AOA control needed for most benefit (-60° to $+60^\circ$ studied)
Demonstrated by others for flight or ground vehicles?	Yes	No
Mechanical implementation difficulty	Easy/moderate	Very difficult
Risk to program if implemented	Low/moderate risk	High risk

IV. Conclusion

Two types of winglet design approaches were considered to create downforce for the Wairua 2 land speed record streamliner: (1) a conventional swept supercritical winglet with variable AOA, and (2) a MSBLC winglet that could operate at various velocity ratios. Due to a limited development timeline the MSBLC concept was studied only as an airfoil at low speeds and was found to greatly enhance lift and delay stall, an effect that was augmented at a higher surface to freestream velocity ratio. MSBLC airfoils could achieve C_L values of 4-5, whereas conventional airfoils achieved no more than approximately 1.6 at best. While similar gains are expected at higher speeds for the MSBLC concept, additional work remains to aerodynamically model MSBLC as a 3D winglet at higher speeds, and design a mechanism and control system capable of operating such a concept. The MSBLC showed great promise, especially due to very high C_L/C_D values, but even the simplest winglet variant needs additional mechanical development and risk mitigation, to include selection and testing of belt materials and design of the drive to power the belt motion. For purposes of upcoming land speed record attempts a conventional supercritical NASA SC(2)-0714 swept winglet design is preferred due to its ease of construction and because CFD simulations have shown its ability to meet the target downforce requirements at multiple speeds. Additional refinement is still possible to reduce the winglet spanwise flow, better streamline the tip endplates, minimize interference drag from the winglet root, and optimize the vortex generators. Work is ongoing for designing a winglet AOA actuation and control mechanism, the structural design of the winglet, and for integrating this winglet into the Wairua 2 vehicle. Although the MSBLC approach was not chosen for Wairua 2, there are ongoing efforts to study its suitability for higher surface and freestream speeds, and for other airfoil variants and vehicles.

Acknowledgments

The authors would like to thank Reg Cook, Chris Stuart, and the entire CMR team for many insightful discussions regarding land speed racing. The views expressed in this article, book, or presentation are those of the authors and do not necessarily reflect the official policy or position of the United States Air Force Academy, the Air Force, the Department of Defense, or the U.S. Government.

References

- [1] Feier, I. I., "Aerodynamic Development of Wairua 1, a 300 MPH Land Speed Record Vehicle," AIAA Paper 2022-1337, January 2022.
<https://doi.org/10.2514/6.2022-1337>
- [2] Feier, I. I., Schwaab, C., and Paillat, G., "Aerodynamic Development of Wairua 2, a 500 mph Land Speed Record Vehicle - Recent Progress, Intake Analysis, and Underbody Shaping," AIAA Paper 2022-1962, January 2022.
<https://doi.org/10.2514/6.2022-1962>
- [3] Modi, V. J., Fernando, M. S. U. K., and Yokomizo, T., "Moving surface boundary-layer control as applied to two-dimensional and three-dimensional bluff bodies," *Journal of Wind Engineering and Industrial Aerodynamics*, Vol. 38, 1991, pp. 83-92.
[https://doi.org/10.1016/0167-6105\(91\)90029-V](https://doi.org/10.1016/0167-6105(91)90029-V)
- [4] Modi, V. J., and Fernando, M. S. U. K., "Moving Surface Boundary-Layer Control: Studies with Bluff Bodies and Application," *AIAA Journal*, Vol. 29, No. 9, 1991, pp. 1400-1406.
<https://doi.org/10.2514/3.10753>
- [5] Modi, V. J., and Yokomizo, T., "On the boundary-layer control through momentum injection: Studies with applications," *Sadhana*, Vol 19, 1994, pp. 401-426.
<https://doi.org/10.1007/BF02812162>
- [6] Modi, V. J., "Moving Surface Boundary-Layer Control: A Review," *Journal of Fluids and Structures*, Vol. 11, 1997, pp. 627-663.
<https://doi.org/10.1006/jfls.1997.0098>
- [7] Modi, V. J., Bandyopadhyay, G., and Yokomizo, T., "High-Performance Airfoil with Moving Surface Boundary-Layer Control," *Journal of Aircraft*, Vol. 35, No. 4, 1998, pp. 544-553.
<https://doi.org/10.2514/2.2358>
- [8] Modi, V. J., "Moving Surface Boundary-Layer Control: A Review," *Journal of Fluids and Structures*, Vol. 11, No. 6, 1997, pp. 627-663.
<https://doi.org/10.1006/jfls.1997.0098>
- [9] Seifert, J., "A review of the Magnus effect in aeronautics," *Prog. in Aerospace Sciences*, Vol. 55, 2012, pp. 17-45.
<https://doi.org/10.1016/j.paerosci.2012.07.001>
- [10] Svorcan J., Wang J. M., and Griffin, K. P., "Current state and future trends in boundary layer control on lifting surfaces," *Advances in Mechanical Engineering*, Vol. 14, No. 7, 2022.
<https://doi.org/10.1177/16878132221112161>
- [11] Kutta, W. M., "Lift Forces in Fluid Flow/Auftriebskräfte in strömenden Flüssigkeiten," *Illustrierte Aeronautische Mitteilungen*, Vol. 6, 1902, pp. 133-135.
- [12] Joukowski, N. E., Collected Works, (in Russian), OGIZ (Association of State Book and Magazine Publishing Houses), State Publ. House of Tech. Theo. Lit., Moscow, Vol. 6, 1950.
- [13] Lafay, A., "Contribution expérimentale à l'aérodynamique du cylindre et à l'étude du phénomène de Magnus," *Revue de Mécanique*, Vol. 30, 1912, p. 417-442.
- [14] Prandtl, L., and Tietjens, O., "Kinetographic Flow Pictures", National Advisory Committee for Aeronautics (NACA) Technical Memorandum, No. 364, 1926. (from "Kinematographische Stromungsbilder", *Die Naturwissenschaften*, Vol. 13, 1925, pp. 1050-1053.)
- [15] Favre, A., "Contribution à l'étude expérimentale de mouvements hydrodynamiques à deux dimensions", Ph.D. dissertation, Université de Paris, France, 1938.
- [16] Salam, M. A., Ali, M. A. T., and Islam, A. Q., "Experimental Analysis of Aerodynamic Performance on asymmetric NACA 23018 Aerofoil incorporating a Leading-Edge Rotating Cylinder", *2020 IOP Conf. Ser.: Mater. Sci. Eng.*, Vol. 912, 2020.
<https://iopscience.iop.org/article/10.1088/1757-899X/912/4/042027>
- [17] Joshi, Y., Kumar, A., Roy, A., and Harichandan, A. B., "Moving Surface Boundary Layer Technique for NACA 0012 Airfoil at Ultra-Low Reynolds Number", *International Journal of Innovative Technology and Exploring Engineering*, Vol. 9, No. 2, 2019, pp. 3788-3795.

- <http://doi.org/10.35940/ijitee.B6299.129219>
- [18] Varghese, J., and Mohammadi, I., “Analysis of the Effect of Moving Surface on 3-D Symmetric Airfoil”, *International Journal of Recent Development in Engineering and Technology*, Vol. 5, No. 8, 2016, pp. 1-8.
https://www.ijrdet.com/files/Volume5Issue8/IJRDET_0816_01.pdf
- [19] Patkunam, K., Sigamani, S., Mahathi, P., and Selvakumaran, T., “Experimental study of Magnus effect over an aircraft wing”, *International J. of Research in Engineering and Technology*, Vol. 4, No. 10, 2015, pp. 406-414.
<https://doi.org/10.15623/ijret.2015.0410066>
- [20] Szulc, O., Doerffer, P., Flaszynski, P., and Braza, M., “Moving wall effect on normal shock wave-turbulent boundary layer interaction”, 57th 3AF International Conference on Applied Aerodynamics, AERO2023-29-SZULC, Bordeaux, France, 2023.
- [21] Lin, M., Lewis, P., and Papadopoulos, P., “Utilising Magnus Effect to Increase Downforce in Motorsport”, *Athens Journal of Technology and Engineering*, Vol. 10, No. 2, June 2023, pp. 123-134.
<https://www.athensjournals.gr/technology/2023-10-2-3-Lin.pdf>
- [22] Sedaghat, A., Badri, M. A., Saghafian, M., and Samani, I., “An Innovative Treadmill-Magnus Wind Propulsion System for Naval Ships”, *Recent Patents on Engineering*, Vol. 8, No. 2, 2014.
<http://dx.doi.org/10.2174/1872212108666140530231724>
- [23] Samani, I., and Sedaghat, A., “A novel MAV with treadmill motion of wing”, *Theoretical and Applied Mechanics Letters*, Vol. 3, No. 6, 2013.
<https://doi.org/10.1063/2.1306202>
- [24] Kazemi, S. A., Nili-Ahmadabadi, M., Sedaghat, A., and Saghafian, M., “Aerodynamic performance of a circulating airfoil section for Magnus systems via numerical simulation and flow visualization”, *Energy*, Vol. 104, 2016, pp. 1-15.
<https://doi.org/10.1016/j.energy.2016.03.115>
- [25] Sentongo, S., Carter, A., Cecil, C., and Feier, I., “Novel Aerodynamic Design for Formula SAE Vehicles”, 70th Annual Meeting of the APS Division of Fluid Dynamics, Vol. 62. No. 14, Nov. 2017.
<https://meetings.aps.org/Meeting/DFD17/Session/E17.3>
- [26] Menter, F. R., “Two-equation eddy-viscosity turbulence modeling for engineering applications”, *AIAA Journal*, Vol. 32, No. 8, 1994, pp. 1598-1605.
<https://doi.org/10.2514/3.12149>
- [27] Wortmann, F. X., “Airfoils With High Lift Drag Ratios at a Reynolds Number of About One Million”, MIT Symposium, in NASA-CR-2315, 1972, pp. 197-204.
<https://ntrs.nasa.gov/citations/19740001939>
- [28] Wortmann, F. X., “The Quest for High-lift”, AIAA Paper No. 74-1018, 1974.
- [29] Sheldahl, R. E., Klimas, P. C., “Aerodynamic Characteristics of Seven Symmetrical Airfoil Section Through 180-Degree Angle of Attack for Use in Aerodynamic Analysis of Vertical Axis Wind Turbines,” Sandia National Laboratories Report SAND90-2114, Albuquerque NM, 1981.
- [30] Abbott, I. H., Von Doenhoff A. E., and Stivers, L., “Summary of Airfoil Data”, NACA-TR-824, 1945.
<https://ntrs.nasa.gov/citations/19930090976>
- [31] Harris, C. D., “NASA Supercritical Airfoils, A Matrix of Family-Related Airfoils”, NASA-TP-2969, 1990.
<https://ntrs.nasa.gov/citations/19900007394>
- [32] Harris, C. D., McGhee, R. J., and Allison, D. O., “Low-Speed Aerodynamic Characteristics of a 14-Percent-Thick NASA Phase 2 Supercritical Airfoil Designed for a Lift Coefficient of 0.7”, NASA-TM-81912, 1980.
<https://ntrs.nasa.gov/citations/19830013896>
- [33] Jenkins, R. V., “NASA SC(2)-0714 Airfoil Data Corrected for Sidewall Boundary-Layer Effects in the Langley 0.3-Meter Transonic Cryogenic Tunnel”, NASA-TP-2890, 1989.
<https://ntrs.nasa.gov/citations/19890008197>
- [34] Englar, R. J., “Experimental Investigation of the High Velocity Coanda Wall Jet Applied to Bluff Trailing Edge Circulation Control Airfoils”, David W. Taylor Naval Ship Research and Development Center, Aviation and Surface Effects Dept., Bethesda MD, Report 4708, 1985.
<https://apps.dtic.mil/sti/tr/pdf/ADA019417.pdf>
- [35] Forster, M., and Steijl, R., “Design study of Coanda devices for transonic circulation control”, *The Aeronautical Journal*, Vol. 121, No. 1243, September 2017, pp. 1368 – 1391.
<https://doi.org/10.1017/aer.2017.65>
- [36] Radwan, S. F., Rockwell, D. O., and Johnson, S. H., “Critical Review of the Training Edge Condition in Steady and Unsteady Flow”, NASA-CR-169705, Lehigh Univ., 1982.
<https://ntrs.nasa.gov/citations/19830006993>